Ehrlichia ruminantium uses its transmembrane protein Ape to adhere to host bovine aortic endothelial cells

Valérie Pinarello[1,2#], Elena Bencurova[3], Isabel Marcelino[4], Olivier Gros[5], Carinne Puech[2], Mangesh Bhide[3,6], Nathalie Vachiery[2] and Damien F. Meyer[1,2*].

[1]CIRAD, UMR ASTRE, F-97170 Petit-Bourg, Guadeloupe, France

[2]ASTRE, CIRAD, INRA, Univ Montpellier, Montpellier, France

[3] Laboratory of biomedical microbiology and immunology, University of veterinary medicine and pharmacy in Kosice, Komenskeho 73, Kosice, Slovakia

[4] Institut Pasteur de la Guadeloupe, 97183 Les Abymes Cedex, Guadeloupe, France

[5] Institut de Systématique, Évolution, Biodiversité (ISYEB), Muséum national d'Histoire naturelle, CNRS, Sorbonne Université, EPHE, Université des Antilles Campus de Fouillole, 97110 Pointe-à-Pitre, France

[6] Institute of neuroimmunology, Slovak academy of sciences, Bratislava, Dubravska cesta 9, Slovakia

[#] present address: CIRAD, UMR ASTRE, Harare, Zimbabwe

*Email: damien.meyer@cirad.fr

Abstract

Ehrlichia ruminantium is an obligate intracellular bacterium, transmitted by ticks of the genus *Amblyomma* and responsible for heartwater, a disease of domestic and wild ruminants. High genetic diversity of *E. ruminantium* strains hampers the development of an effective vaccine against all strains present in the field. In order to develop strategies for the control of heartwater through both vaccine and alternative therapeutic approaches, it is important to first gain a better understanding of the early interaction of *E. ruminantium* and its host cell. Particularly, the mechanisms associated with bacterial adhesion remain to be elucidated. Herein, we studied the role of *E. ruminantium* membrane protein ERGA_CDS_01230 (UniProt Q5FFA9), a probable iron transporter, in the adhesion process to host bovine aortic endothelial cells (BAEC). The recombinant version of the protein ERGA_CDS_01230, successfully produced in the *Leishmania tarentolae* system, is O-glycosylated. Following *in vitro* culture of *E. ruminantium* in BAEC, the expression of CDS ERGA_CDS_01230 peaks at the extracellular infectious elementary body stages. This result suggest the likely involvement of ERGA_CDS_01230, named hereafter Ape for Adhesion protein of *Ehrlichia*, in the early interaction of *E. ruminantium* with its host cells. We showed using flow cytometry and scanning electron microscopy that beads coated with recombinant ERGA_CDS_01230 (rApe) adheres to BAEC. In addition, we also observed that rApe interacts with proteins of the cell lysate, membrane and organelle fractions. Additionally, enzymatic treatment degrading dermatan and chondroitin sulfates on the surface of BAEC is associated with a 50% reduction in the number of bacteria in the host cell after a development cycle, indicating that glycosaminoglycans seem to play a role in the adhesion of *E. ruminantium* to the host cell. Finally, Ape induces a humoral response in vaccinated animals. Globally, our work identifying the role of Ape in *E. ruminantium* adhesion to host cells makes it a gold vaccine candidate and represents a first step toward the understanding of the mechanisms of cell invasion by *E. ruminantium*.

Introduction

Ehrlichia ruminantium is an obligate intracellular Gram-negative bacterium responsible for the fatal and neglected heartwater disease of domestic and wild ruminants (Allsopp, 2010). This bacterium belongs to the Anaplasmataceae family in the order Rickettsiales that includes many pathogens and symbionts of veterinary and public health importance (Moumene and Meyer, 2015). *E. ruminantium* is transmitted by ticks of the genus *Amblyomma* in the tropical and sub-Saharan areas, as well as in the Caribbean islands. It constitutes a major threat for the American livestock industries since a suitable tick vector is already present in the American mainland and potential introduction of infected *A. variegatum* through migratory birds or uncontrolled movement of animals from Caribbean could occur (Deem, 1998), Kasari et al., 2010). The disease is also a major obstacle to the introduction of animals from heartwater-free to heartwater-infected areas into sub-Saharan Africa and thus restrains the breeding to upgrade local stocks (Allsopp, 2010). The small genome of *E. ruminantium* (1.5 Mb) shows an unique process of contraction/expansion in non-coding regions and targeted at tandem repeats (Frutos et al., 2006). This genome plasticity, associated with a high genetic diversity, suggests a capacity of adaptation upon exposure to a novel environment and could also explain the low field efficacy of available vaccines (Cangi et al., 2016).

After adhesion and entry of infectious elementary bodies into host cells, *E. ruminantium* replicates by binary fission of reticulated bodies into an intracellular vacuole bounded by a lipid bilayer membrane derived from the eukaryotic host endothelial cell membrane (Dumler et al., 2001). *Ehrlichia* spp. have evolved sophisticated mechanisms to invade and multiply in host tissues by hijacking/subverting host cell processes ranging from host signaling, modulation of vesicular traffic, protection from oxidative burst, acquisition of nutrients, and control of innate immune activation (Moumene and Meyer, 2015). Notably, *E. chaffeensis* secretes the type IV effector Etf-1 to induce autophagy and capture nutrients, whereas it uses Etf-2 to delay endosome maturation to avoid phagolysosomal fusion for the benefit of bacterial replication (Lin et al., 2016;Yan et al., 2018). Moreover, recent work identified that *E. chaffeensis* uses EtpE invasin to enter mammalian cells via the binding to its receptor DNaseX, a glycosylphosphatidylinositol-anchored cell surface receptor (Mohan Kumar et al., 2013). That receptor-triggered entry simultaneously blocks the generation of reactive oxygen species (ROS) by host monocytes and macrophages (Teymournejad et al., 2017).

Due to the lack of some key metabolic genes that are required for host-free living and similarly to what is observed in other intracellular bacteria, entry into the eukaryotic host

82 cells is crucial for *E. ruminantium* to sustain its life and disseminate (Pizarro-Cerda and
83 Cossart, 2006) ; (Frutos et al., 2007). Computational studies have predicted type IV effectors
84 in *E. ruminantium* (Noroy et al., 2019) which, however, remain to be characterized; the
85 mechanisms of adhesion and entry are still unknown and may be active or passive
86 depending on the pathogen. . *E. ruminantium* could either inject a type IV effector across
87 the host cell membrane to trigger actin rearrangement and pathogen phagocytosis such as
88 *Bartonella henselae* (Truttmann et al., 2011). An another option is the use of homologous
89 system of *E. chaffeensis* invasion/receptor pair (Mohan Kumar et al., 2013) or an outer
90 membrane protein of the OmpA family that actively trigger internalization as was observed
91 in *Coxiella burnettii* (Martinez et al., 2014).
92 Bacterial pathogens are capable of exploiting and diverting host components such as
93 proteoglycans for their pathogenesis (Aquino et al., 2018). These assemblies of
94 glycosaminoglycans (GAGs) chains fixed around a protein nucleus (Bartlett and Park, 2010)
95 are expressed constitutively on the cell surface, in intracellular compartments as well as in
96 the extracellular matrix. They are known to act as receptors for pathogens in many cases of
97 infection (Aquino et al., 2018); (Rajas et al., 2017); (Gagoski et al., 2015). Many pathogens
98 – *e.g. Chlamydia trachomatis* with a biphasic life cycle like *E. ruminantium* – use GAGs as
99 an initial anchor site of low affinity; this facilitates interaction with their respective secondary
100 receptor allowing internalization but GAGs are sometimes also used as bridging molecules
101 (Aquino et al., 2010). Thus, whether *E. ruminantium* uses GAGs as a portal of entry or any
102 specific bacterial surface protein is unknown but essential for developing any anti-infective
103 measures.
104 The outer membrane proteome study of *E. ruminantium* Gardel strain revealed that a
105 hypothetical protein, the possible major ferric iron binding protein precursor the putative iron
106 transporter ERGA_CDS_01230, is uniquely expressed in the outer-membrane fraction
107 (Moumene et al., 2015). This protein was also shown to be O-glycosylated only in *E.*
108 *ruminantium* (Marcelino et al. 2019). Moreover, homologous counterparts of this protein in
109 other pathogenic species play a key role in bacterial survival within the host by scavenging
110 iron from mammalian serum iron transport proteins (Brown et al., 2010). Interestingly, we
111 previously showed that iron starvation induces expression of virulence factors such as type
112 IV secretion genes (Moumene et al., 2017).
113 In this study, we show that ERGA_CDS_01230 (UniProt Q5FFA9, named herein Ape for
114 Adhesion protein of *Ehrlichia ruminantium*,) is involved in the binding of *E. ruminantium* to
115 bovine aortic endothelial cells (BAEC). In order to study whether Ape alone can mediate the

116 invasion of host cells by adhering to endothelial cells membrane, we used latex beads
117 coated with recombinant Ape. These beads covered with the protein adhered and seemed
118 to enter endothelial cells similarly to what is observed with *E. ruminantium in vitro* (Moumene
119 and Meyer, 2015). Subsequent investigation uncovered that rApe is a glycosylated protein
120 that induces a strong humoral immune response in vaccinated goats making it a possible
121 vaccine candidate.
122

123 ## Methods

124 **Synchronous culture**

125 *E. ruminantium* (strain Gardel) was propagated in Bovine Aortic endothelial cells (BAEC
126 isolated at CIRAD, Guadeloupe, France) in Baby Hamster Kidney (BHK-21) cell medium
127 supplemented with 1% L-glutamine 200mM (Eurobio), 10% heat-inactivated fetal bovine
128 serum (FBS, Thermofisher), 1% penicillin 10000UI/ streptomycin 10000 µg (Eurobio), 1x
129 amphotericin B (Sigma), 5% NaHCO3 5.5%, under 5% CO_2 at 37°C modified from
130 (Marcelino et al., 2005). The cell trypsinization (Trypsin-Versen, Eurobio) was carried out
131 with a splitting ratio of ½ when monolayer reached 100% confluence. Synchronous infection
132 of a new BAEC monolayer was obtained using a bacterial suspension previously harvested
133 at 120 hpi by scraping the TC flask (TCF) and passing infected lysed cells through 18G and
134 26G needles before reinfection at a ratio of 1/20 (Marcelino et al., 2005).
135

136 **Quantitative reverse transcription RT-PCR along bacterial cycle**

137 *E. ruminantium*-infected BAE cells were harvested for RNA extraction by trypsinization at
138 24, 48, 72 and 96 hours post infection (hpi), centrifuged 1700 x g, 5 min at 4°C and by cell
139 lysate scrapping at 120 hpi, centrifuged 20000 x g, 15 min at 4°C. All pellets were dissolved
140 in 1 mL TRIZOL (Thermofisher), RNA was extracted following manufacturer's
141 recommendations and eluted in 100 µL H_2O RNase/DNase free. RNA was treated by Turbo
142 DNAse (Ambion) according to supplier's instructions and precipitated overnight at -20°C in
143 2.5 volume (v/v) cold absolute ethanol (Normapur), 1/10 volume of 3 M sodium acetate and
144 1 µL glycogen 10 mg/mL (Thermofisher). Pellet obtained by centrifugation 15000 x g, 10
145 min, 4°C was washed with 1 mL 75% ethanol, air dried after centrifugation 9000 x g, 7 min,
146 4°C and dissolved in 20 µL H_2O RNase/ DNase free. Two µg ARN were reverse transcribed
147 using "SuperScript™ VILO™ cDNA Synthesis Kit" (Invitrogen), according to the supplier's
148 specifications.

149 **Pre amplification of *ape* gene**

150 Quantification started by 15 cycles of pre-amplification (same reaction mix and cycling
151 conditions as below). ERGA_CDS_01230 (Ape) was amplified in 25 µL reaction mix
152 containing 250 nM of the forward ERGA_CDS_01230F AATGGAGAATGAGGGGGAAG
153 and reverse ERGA_CDS_01230R ACCCAAACCAAAATCCATCA primers, 12.5 µL of
154 Power SYBR® Green PCR Master Mix (Thermofisher), 12.5 µL H_2O RNase/ DNase free
155 and 20 µL pre-amplified DNA. Reactions were performed in a Quantstudio 5 (Thermofisher)
156 as follow: 50°C, 2 min for Uracil-N-Glycosylase activation, 95°C, 10 min for Uracil-N-
157 Glycosylase inactivation and polymerase activation; 40 cycles 95°C, 15 sec denaturation
158 and 59°C, 60 sec hybridization and elongation. The specificity of the PCR product was
159 confirmed by the dissociation curves.

160 **Quantification of *E. ruminantium* along the bacterial cycle**

161 *E. ruminantium* quantification for normalization as described by (Pruneau et al., 2012), was
162 performed by DNA extraction according to manufacturer's specifications (QiaAmp DNA
163 minikit, QIAGEN, Courtaboeuf) on 1/10 of the harvested volume, after 20000 x g, 15 min
164 centrifugation and dissolution in 200 µL PBS 1x, followed by a quantitative polymerase chain
165 reaction (qPCR) *Sol1* targeting the pCS20 region (Cangi et al., 2017).

166 **Normalization of *ape* gene expression**

167 Normalization by *E. ruminantium* quantification was calculated: *Rx hpi= [cDNA copy number*
168 *$_{(ERGA_CDS_01230)}$] / [E. ruminantium pCS20 DNA copy number]*, allowing fold change (FC)
169 determination, compared to expression at 96 hpi (corresponding to the stationary phase of
170 the bacterial growth): FC = $R_{x\ hpi}$/ $R_{96\ hpi}$. Results were represented in log2, according to
171 Pruneau et al. (2012) and confirmed by 2 others biological replicates (data not shown).

172

173 **Recombinant protein production**

174 pLEXSY_I-blecherry3 plasmid (Bioscience, 2011) and 400 ng of amplified
175 CDS_ERGA_01230 were digested 10 min at 37°C by BamHI and SalI (Thermo Scientific,
176 USA) and column purified (Macherey Nagel, Germany). The digested product was ligated
177 in pLEXSY_I-blecherry3 plasmid using T4 DNA Ligase (Thermo Scientific) for 1 h at 22°C.
178 pLEXSY_I-blecherry3 plasmid was modified with the addition of a sequence coding GFP at
179 C-terminus of the insert and 6X His tags at N-terminus of insert. It is to note that, GFP and
180 the coding sequence of CDS_ERGA_01230 were linked with the sequence encoding
181 cleavage site for Xa factor. Ligated plasmid was column purified and 50 ng of the ligation
182 mix was electro-transferred to competent bacteria *E. coli* XL10 (Miller and Nickoloff, 1995).

183 100 µL of transformed culture were spread on LB medium Petri dish supplemented with
184 carbenicillin (50µg/ml). To confirm the presence of the plasmid and the insert, a PCR was
185 performed on a colony using vector specific primers (Forward,
186 CGCATCACCATCACCATCACG; Reverse, ACCAAAATTGGGACAACACCAGTG). PCR
187 product was then sequenced. Transformed E. coli clone was grown 16 h at 37°C under 200
188 rpm stirring until optical density (OD) reached 3. The plasmid was isolated
189 using "GenElute™ Plasmid Midiprep" kit (Sigma Aldrich) and digested with *SmaI* (Thermo
190 Scientific)
191 *Leishmania tarentolae* preculture was grown in 10 mL LEXSY BHI medium with TC flask at
192 26°C. 3 days after, preculture was diluted 10 fold in 10 mL LEXSY BHI medium and
193 incubated overnight at 26°C (flat position). Next day, *Leishmania tarentolae* were
194 centrifuged 5 min (2000 x g) and half of the medium was removed. Cells were resuspended
195 in remaining medium to get 10^8 cells/ mL and incubated 10 min on ice. 350 µL cells were
196 electroporated at 450 V, 450 µF, 5 - 6 msec impulsions with 5 µg linearized plasmid (smal
197 digested). Cells were immediately incubated for 10 min on ice, transfer to 10 mL LEXSY BHI
198 medium (Bioscience) and incubated overnight. 10 µL bleomycin (100 mg/mL, (Bioscience)
199 was then added to nonclonal selection for 3 more days. 5 mL of culture supernatant was
200 centrifuged for 3 min at 1000 x g. Pellet was resuspended in 10 mL LEXSY BHI medium
201 containing bleomycin and incubated at 26°C for 5 days. After nonclonal selection,
202 expression of protein was induced in 45 mL BHI medium supplemented with bleomycin and
203 tetracyclin 10 mg/mL (Bioscience). 5 ml of culture from nonclonal selection was added
204 incubated for 72 h at 26°C with shaking at 100 rpm. Supernatant was harvested and
205 concentrated in dialyses bag (3.5 kDa membrane, Serva) in a polyethylene glycol solution
206 20000 overnight at 4°C. Proteins were concentrated and purified by Sephadex gel filtration.
207 **Mass spectrometry analysis**
208 Protein size was verified by MALDI-TOF (Microflex, Bruker). The presence of GFP tag and
209 associated fluorescence was checked respectively by immunoblotting and aggregation on
210 Probond beads followed by fluorescence microscopy. Mass spectrometry allowed to check
211 rApe size and Orbitrap allowed to confirm identity of the protein.
212
213 **3D Structure and localization prediction**
214 Protein structure prediction was accomplished using I-TASSER-MTD (Xiaogen Zhou,
215 2022)and view was generated by MacPyMol (DeLano, 2009). The subcellular localization
216 was predicted by "CELLO 2.5: subCELlular LOcalization predictor" (Yu et al., 2006), from

217 the protein sequence, accession number CAI27575.1. Ape structural homology was
218 determined using “Swiss model, Expasy” (Waterhouse et al., 2018).
219
220 **Western Blot for O-GlcNac Glycoprotein detection**
221 rApe was migrated on an acrylamide gel "SDS page" (NuPAGE bis-tris, Novex) for 2 h 30
222 min at 100V and 400mA in MOPS buffer (Novex), according to the supplier's instructions
223 (Nu PAGE Technical Guide). Approximately 10 µg protein and BSA for the negative control
224 were denatured at 70°C for 10 min with LDS buffer and reducing agent (Novex) and migrated
225 with a 3 to 198 kDa molecular weight marker (SeeBlue plus 2, Invitrogen). A gel-sized PVDF
226 membrane (Amersham, Hybond-P) was soaked for 30 sec in methanol (Normapur) and
227 incubated in transfer buffer (20x, NuPAGE) for at least 15 min with the same size filter
228 papers (Whatman) and 4 sponges. The transfer assembly was performed according to the
229 NuPAGE technical guide and the transfer was run 1 h 15 min at 30 V, 170 mA. The
230 membrane was then immersed in a solution of Culvert Red (AMRESCO) ~1 min and rinsed
231 with water prior to picture. The protocol for western blot detection was modified from
232 (Marcelino et al., 2019).The membrane was blocked for 3 h at room temperature (RT) with
233 stirring in PBS (pH 7.4), 0.05% Tween20 (PBS-T) and 5% milk. Then, membrane was
234 incubated overnight with anti-O-GlcNAc antibody (Santa Cruz), monoclonal IgM, diluted 200
235 fold in blocking solution. After three washes with PBS-T, membrane was incubated with anti-
236 mouse antibody (IgM-HRP, Molecular probes) diluted 1000 fold in PBS-T for one hour. The
237 membrane was washed 3 times 10 min with PBS-T before the addition of the TMB substrate
238 (Pierce) and gel reader picture once the color was developed.
239
240 **Glycosaminoglycans degradation assays**
241 10, 5, 1 and 0.3 µg/ mL heparan sulfate (Jonquieres et al., 2001;Kobayashi et al., 2010) and
242 9 µg/ mL rApe (positive control) were adsorbed in 50 µL of carbonate/bicarbonate buffer pH
243 9.6 (Martinez et al., 1993), distributed in Nunc Maxisorp wells, 1 h at 37°C with gentle stirring
244 then overnight at 4°C. The next day, 3 washes were carried out with 200 µL of PBS-T per
245 well. Blocking was done 1 h at 37°C under agitation with 100 µL of blocking buffer PBS
246 tween 20 0.05% milk 3%, followed by 3 washes with 200 µL of PBS-T per well. 50 µL/ well
247 of rApe at 14.3 µg/mL diluted in PBS tween 20 0.05% milk 3% was incubated 1 h at 37°C
248 with stirring. Three washes of 200 µL PBS-T per well were performed, followed by addition
249 of 50 µL anti-GFP antibody diluted to 4,000 in PBS-T with milk 3% and incubation 1 h at
250 37°C with stirring. Washings were repeated as above. Addition of 200 µL TMB substrate

251 allowed revelation within 30 min at 37°C before to stop the reaction with 100 µL of H2SO4
252 2N. The reading was done at 450 nm (Multiskan, Thermofisher). 2 cm^2 wells were inoculated
253 with ~$1.1x10^4$ BAEC in 500 µL BHK21 medium. When confluence was reached, several
254 concentrations of chondroitinase (Sigma Aldrich) were tested as follows: 0.2U, 0.4U and
255 0.9U/ mL chondroitinase was incubated 2 h before infection with the BAEC in 1X PBS and
256 bovine fetal serum (SBF)-free BHK21 medium (Sava et al., 2009;Rajas et al., 2017). The
257 medium was renewed with standard BKH21 prior infection at a ratio 1/20 and 2 h after
258 infection. At lysis stage, all the wells were scraped, centrifuged for 15 min at 20,000 x g.
259 DNA was extracted using the QiaAmp DNA minikit (Qiagen) and quantified using qPCR™
260 Sol1, targeting the pCS20 region (Cangi et al., 2017). The results were treated using the
261 ΔΔCt method and represented in $2^{-\Delta\Delta Ct}$.
262
263 **Flow cytometry for attachment quantification**
264 We used the cytometer to quantify the fluorescence-labelled cells following incubation with
265 rApe. Six-well Nunc plates (9.6 cm^2/ well) with confluent BAEC were incubated for 2 h at
266 37°C, 5% CO_2 with rApe concentrations ranging from 6.4 to 102.4 µg/ mL following the
267 principle described in (Lundberg et al., 2003). The negative control consisted of confluent
268 BAE cells. After incubation with recombinant protein, each well was rinsed twice with 1 mL
269 of 1X PBS and 1.5 mL of 1X PBS was used to scrape the well. After centrifugation during
270 10 min at 200 x g, at 4°C cells were resuspended in Isoflow (Beckman) for further reading
271 the percentage of fluorescent labelled cells on the cytometer (FC500, Beckman Coulter).
272
273 **Far Western Blot**
274 The BHK21 culture medium of a 175 cm^2 TCF was removed, the TCF was washed with 5mL
275 of PBS 1x containing anti-protease (Roche). ~10mL of cold PBS 1x was added to gently
276 scrap the cell mat. Centrifugation 10 min at 200 x g and 4°C was performed to remove the
277 supernatant. Lysis of the pellet was performed by addition of 3 mL native lysis buffer (150
278 mM NaCl, 50 mM Tris-HCl, pH 7.4, NP-40 1%, anti-proteases 1%), followed by 4
279 "freeze/thaw" cycles by first immersing the lysate 2 min in an ethanol/ ice bath, then 2 min
280 in a 37°C water bath. The lysate was vortexed between each bath. The cells were broken
281 by passing the lysate 4 times through an 18G needle with a syringe. The cell debris were
282 pelleted at 10000 x g for 30 min prior to supernatant transfer into a new tube.
283 Four different fractions (F1, cytosol components; F2, membrane and organelle components;
284 F3, nucleus components; F4, the cytoskeleton) were extracted using the "ProteoExtract

285 Subcellular Proteome Extraction kit" (Calbiochem/ MERCK) according to the supplier's
286 instructions. Each fraction was placed in acetone (at least 5x the volume of the extracted
287 fraction) for overnight precipitation at -20°C. The day after, each pellet was re-suspended in
288 500µL of native lysis buffer after 20 min centrifugation at 15000 x g and 4°C.
289 18 µL of each cell fraction and 35 µL of lysate were migrated onto acrylamide gel, with
290 addition of LDS, under the same conditions as for the glycosylation tests (but without
291 addition of reducing agent or heating), as well as for the transfer onto PVDF membrane.
292 The membrane was stored in TTBS 1x (10mM TRIS, 150mM NaCl, 0.05% Tween 20, pH
293 8,3), then blocked for 1 h at RT under gentle agitation in 2% Bovine Serum Albumine (BSA)
294 in TTBS and finally rinsed 3 times for 5 min with TTBS. The membrane was incubated
295 overnight at 4°C under slow rotation with 0.5 mg rApe in 1% BSA in TTBS. The negative
296 control (without recombinant protein) was incubated in the same conditions. The next day,
297 the membrane was washed 3x for 5 min with TTBS and incubated 1 h at RT under agitation
298 with anti-GFP-HRP (Thermofisher) diluted 2,500 fold in 1% BSA in TTBS. The membrane
299 was washed again 3 x for 5 min with TTBS. The binding of anti- GFP-HRP was revealed by
300 the addition of 4.5 mL peroxide substrate (Pierce Thermofisher) + 0.5mL chromogen DAB
301 (Thermofisher) and incubation 10 min at RT. Picture was taken by colorimetry reading.
302
303 **Scanning electronic microscopy for binding assays**
304 Two kinds of fluorescent latex beads (with a sulfate group) were adsorbed with rApe through
305 electrostatic interactions based on (Martinez et al., 2014). A total of 10^{10} beads (0.1 µm in
306 diameter) and $7x10^9$ beads (0.5 µm in diameter) were adsorbed with 100 µg/mL rApe in 1
307 mL of 25 mM MES, pH 6.1 (Sigma Aldrich) during 4h at RT under slow rotation. Then, three
308 washes were performed using the same buffer before to be resuspended in 1 mL of 1% BSA
309 MES. 24-well plates containing 13 mm diameter lamellae (VWR) were inoculated with
310 BAEC. A deposit of 0.1 or 0.5 µm-diameter beads ($1.82x10^8$ per well) was made in BHK21
311 medium. The negative control consisted of recombinant protein-free beads incubated with
312 BAEC. The plate was centrifuged 5 min at 200 x g at RT before incubation 30-120 min at
313 37°C under 5% CO_2 atmosphere. Three washes with PBS 1X removed the excess of
314 unbound beads before overnight fixation with 2% paraformaldehyde. Lamellae were then
315 removed from each well and dehydrated in series of acetone solutions of increasing
316 concentration, dried to critical point in CO_2 and sputter-coated with gold before observation
317 with a FEI Quanta 250 electron microscope at 20 kV.
318

319 **ELISA-based binding assays**

320 The antibody response to Ape during vaccination of goats was tested by ELISA. Sera for
321 vaccinated goats obtained from previous studies (Marcelino et al. 2015 a, b) were incubated
322 in wells coated with rApe, followed by incubation with anti-goat IgG antibody coupled to
323 HRP.

324 The adsorption of 4 µg/ mL rApe diluted in 100 µL of carbonate bicarbonate buffer pH 9.6
325 was performed in a Nunc plate (Maxisorp). One hour incubation was carried out at 37°C with
326 stirring at 150 rpm then overnight at 4°C. The plate was washed with 300 µL/ well of wash
327 buffer (PBS 1x pH 7.2, Tween 20 0.1%). Blocking was carried out at 37°C with stirring in
328 300 µL blocking buffer (PBS1x, tween 20 0.1%, casein 2%) for 1 h. Washings were repeated
329 as described in the previous step. 100 µL of each goat serum diluted 100-fold in blocking
330 buffer was incubated 1 h at 37°C with agitation (Perez et al., 1998); 2 blank wells were
331 incubated with 100 µL blocking buffer. Five washes with Wash Buffer preceded the deposit
332 of 100 µL of anti-goat IgG antibody (Rockland) diluted 20,000-fold in blocking buffer and 1
333 h incubation at 37°C with agitation. Five washes were performed. The revelation was
334 performed by addition of 100 µL of TMB (Neogen) and stopping of the reaction after 5 min
335 development by the addition of 50 µL of 0.5 M H_2SO_4. Antibody response was detected by
336 ELISA titers and optical density (OD) was read with a spectrophotometer at 450nm. The OD
337 of the wells without serum were valid when < 0.1 ; OD of negative samples were valid when
338 < 0.2.

339

340 **Results**

341

342 **ERGA_CDS_01230 (*ape*) is highly expressed at infectious elementary body stages of**
343 ***E. ruminantium* development inside mammalian cells**

344 In order to measure the expression of the *ape* gene, normalization was carried out in relation
345 to the number of bacteria present at each stage of development since no reference gene
346 with a sufficiently stable expression is available for *E. ruminantium*. The development cycle
347 of *E. ruminantium* is synchronized when the lysis occurs 5 days after BAEC infection.
348 Quantification of the number of bacteria present in the BAEC every 24 hpi by qPCR Sol1
349 showed a sigmoidal curve represented in log10 (Figure 1A). The bacterium had a slow
350 growth phase between 24 and 48 hpi then an exponential development with a slowing down
351 of the growth, a stationary phase after 96 hpi and a maximum of copies reached at 120 h
352 (release of elementary bodies). The number of transcripts was determined by qPCR and a

353 ratio calculated at each time as follow: (*E. ruminantium* $_{\text{cDNA number}}$) / (*E. ruminantium* $_{\text{pCS20}}$
354 $_{\text{DNA copy number}}$). The fold change (FC) was determined in relation to bacterial expression at 96
355 hpi (stationnary phase) and represented graphically in Figure 1B. The expression of *ape*
356 gene peaks at the elementary body infectious stages of *E. ruminantium* life cycle which
357 correspond to 120 hpi (host cell lysis) and 24 hpi (lag phase). These data indicate that *ape*
358 is expressed when the bacterium is released and ready to infect new cells.
359

360 **Ape protein presents a C-clamp structure and is predicted to be an outer-membrane**
361 **protein**

362 The 3D structure proposed by I-TASSER-MTD software (Figure 2A) showed that Ape
363 harbours a succession of helixes α linked by loops distributed around a β sheet and showed
364 a "c-clamp" three-dimensional structure. By homology with other known I^{ry}, II^{ry} or III^{ry}
365 structures, "Swiss model" showed a strong analogy of Ape with a "C-clamp" structure,
366 capable of binding iron. According to the "CELLO 2.5" software, Ape has a dominant
367 cytoplasmic localization (score of 2.418) but is also present at the outer membrane (1.652)
368 (Figure 2B). This canonical sub-cellular localization of a transmembrane protein is in
369 accordance with previous results finding this protein in the outer membrane proteome
370 (Moumene et al., 2015).
371

372 **rApe protein shows O-glycosylated post-traductional modifications**

373 Western blot analysis showed that rApe was detected with an anti-O-GlcNAc antibody at the
374 expected size of 66kDa (Figure 3). This size confirmed the data obtained by mass
375 spectrometry and is 30% larger than the one estimated by the amino acid sequence
376 encoded by *ape* gene (41 kDa for 365 amino acids). The identity of rApe protein sequence
377 blasted with the possible major ferric iron binding protein precursor (Q5FFA9). Altogether
378 these results demonstrate the O-glycosylation of rApe.
379

380 **Enzymatic treatment of BAEC with chondroitinase decreases invasion by *E.***
381 ***ruminantium***

382 To investigate whether GAGs have a role in *E. ruminantium* adhesion process, BAEC were
383 treated with chondroitinase and then infected with *E. ruminantium*. The number of bacteria
384 was calculated at the end of growth, during the lysis of the BAEC, by qPCR Sol1 for each
385 treatment. After treatment with chondroitinase at 0.2U/mL, the FC corresponding to the
386 bacterial amount differential was higher than for the condition without treatment but this may

387 be explained by inter-well variability (Figure 4). Increasing chondroitinase concentrations to
388 0.4 and 0.9U/mL resulted in FC of 0.52 and 0.58, respectively, corresponding to a 50%
389 reduction of the number of bacteria compared to the untreated condition, highlighting the
390 role of chondroitin sulfate and dermatan sulfate in adhesion of *E. ruminantium* to the cell.
391 No affinity of rApe for heparan sulfate could by revealed using HRP anti-GFP antibody (data
392 not shown).
393
394 **rApe binds to BAEC**
395 To go further in the understanding of the role of Ape in *E. ruminantium* invasion of host cells,
396 we analyzed the interaction of rApe with the surface of endothelial cells using flow cytometry.
397 Adhesion of recombinant proteins to BAEC was measured using flow cytometry to detect
398 the fluorescence of rApe harboring GFP tag. The dot plot profile clearly showed that the
399 percentage of labelled BAEC with rApe increases with the amount of rApe protein (Figure
400 5). As a negative control, the auto-fluorescence of the cells was measured on cells without
401 recombinant protein incubation. The percentage of labelled cells increased with protein
402 concentration up to 36 µg, showing a dose-effect relationship. Above these concentrations,
403 bending of the curve starts with 50% of rApe labelled BAE.
404
405 **Ape interacts with BAEC lysate, membrane and organelles cell fractions**
406 The Far Western blot shows the interaction between rApe and the cell fractions as well as
407 the lysate of the BAEC. rApe interacted with proteins of the cell lysate and more specifically
408 with those of the membrane and organelle fraction (Figure 6).
409
410 **rApe coated beads adhere to BAEC and start internalization mechanism**
411 The visualization of interaction between rApe and the host cell was possible through usage
412 of beads adsorbed with rApe (mimicking *E. ruminantium*) and incubated with BAEC.
413 Adhesion was evaluated by scanning electron microscopy. The negative control showed
414 that non-coated beads did not adhere to the surface of the BAEC, that harbor their classical
415 fried egg shape (Figure 7A). In contrast, Figure 7B showed swollen BAEC, dotted with rApe
416 adsorbed beads after 30 minutes incubation, revealing an interaction between rApe and the
417 BAEC. Figure 7C displayed that rApe-coated beads also adhere (black arrow) and begin to
418 be invaginated (white arrow) by the endothelial cell membrane. Beads diameter did not
419 affect interaction of rApe and the BAEC. The images shown are representative of the
420 observations made in other fields. These data reinforcing the results obtained by

421 immunoblotting and flow cytometry prove that Ape interacts with the host cell membrane
422 and is involved in the adhesion of *E. ruminantium* to the host cell.
423
424 **Ape induces an antibody response in vaccinated goats**
425 In order to verify if *E. ruminantium* Ape protein induces a humoral response following
426 vaccination in goats, we tested sera from *in vivo* experiments on animals vaccinated with an
427 inactivated or attenuated bacterial vaccine (Marcelino et al. 2015 a, b). Goats #614 and #915
428 were both naïve prior to vaccination, characterized by the absence of antibodies against
429 Ape at 3 and 5 weeks post-vaccination, respectively (Figure 8). For #915, the ELISA test
430 showed an increase in humoral response against rApe over time. In fact, the antibody
431 response was developing between 5 and 7 weeks post-vaccination, the latter corresponding
432 to the vaccine boost. For goat #614, inoculation of an attenuated bacterial vaccine also
433 conduced to a humoral response, including response against rApe. These results suggest
434 that rApe could be a relevant target for further studies to see whether it could be a protective
435 immunogen in *E. ruminantium* infection *in vivo.*
436
437 ## Discussion
438 Controlled and determined *Ehrlichia* entry into host cell is a fundamental first step for an
439 effective infectious developmental cycle, particularly for an obligate intracellular pathogen
440 that strictly relies on its host to grow. In the last decade, comparative genomics and cellular
441 microbiology allowed major discoveries in the molecular pathogenesis of Anaplasmataceae.
442 These integrated approaches led to the effective identification of several bacterial virulence
443 determinants (*e.g.* effectors and regulators) and their diverse mechanisms of action
444 (Martinez et al., 2005;Cheng et al., 2008); (Rikihisa, 2017); Marcelino et al., 2015b ;
445 (Moumene et al., 2017). Notably, Rikihisa *et al.* identified that the EtpE protein governs the
446 binding and entry of *E. chaffeensis* into its host cells (Mohan Kumar et al., 2013). The binding
447 of EtpE to DNaseX elicits a signaling cascade that results in cytoskeleton modification,
448 filopodial induction and finally endocytosis into the host cell (Green et al., 2020). Previous
449 studies demonstrated that functional conservations of molecular pathogenicity determinants
450 can occur between of *E. chaffeensis* and *E. ruminantium* (Moumene et al., 2017) but such
451 bacterial ligand was still unknown in *E. ruminantium* at the beginning of this study. Among
452 other Rickettsiales, a receptor-mediated endocytosis was only reported for *Rickettsia conorii*
453 (Moumene et al., 2017) ; (Martinez et al., 2005).

454 Our aim being to determine some major pathogenicity determinants of *E. ruminantium*, we
455 chose to analyze ERGA_CDS_01230 (Ape, UniProt Q5FFA9), a putative iron-transporter
456 previously identified in the outer-membrane proteome of *E. ruminantium* (Moumene et al.,
457 2015). Indeed, we postulated that some key bacterial proteins involved in the early
458 interaction with the eukaryotic host cell should be overexpressed at early stages of the
459 developmental cycle and at the bacterial-host interface. Moreover, we previously showed
460 that iron was a triggering environmental cue for several *E. ruminantium* molecular virulence
461 determinants. Indeed, iron depletion induced a master regulatory gene, genes encoding
462 outer-membrane proteins of the Map1 family and genes of the Type IV Secretion System, a
463 major bacterial pathogenicity determinant (Moumene et al., 2017). Therefore, taking into
464 account that iron is a virulence triggering signal of *Ehrlichia,* Ape protein being a putative
465 iron transporter made it an excellent candidate for further characterization. In the present
466 study, we focused on the role of Ape protein in the interaction between *E. ruminantium* and
467 its mammalian host cell, notably during adhesion. As depicted in our working model for *E.*
468 *ruminantium* binding and invasion of its host endothelial cell (Figure 9), we showed that Ape
469 epitopes are recognized by the immune system of goats vaccinated with live attenuated
470 strain or killed strain or *E. ruminantium*. Indeed, after vaccination, we detected Ape
471 antibodies in sera of vaccinated goats indicating a global humoral response. Following this
472 model, the initial binding of *E. ruminantium* onto the host cell surface seems to involve
473 glycosaminoglycans (GAGs) as chondroitinase treatment of BAEC resulted in a significant
474 decrease of the number of bacteria present at the end of development cycle. The *ape* gene
475 is highly expressed at the elementary body developmental stages of *E. ruminantium*,
476 particularly during host cell lysis which precedes *E. ruminantium* release from host cells to
477 initiate a new cycle of infection. Interestingly, recombinant protein rApe is an O-glycosylated
478 protein that interacts with cell membrane and latex beads coated with rApe were able to
479 adhere to the BAEC surface to initiate internalization and follows a similar pattern of entry
480 like that of *E. ruminantium* (Moumene and Meyer, 2015).
481 Our results showed that Ape protein, an *Ehrlichia* ligand different from previously identified
482 *E. chaffeensis* EtpE (Mohan Kumar et al., 2013), is important for *E. ruminantium* adhesion
483 to the mammalian host cells. The mechanisms used by *E. ruminantium* to invade its host
484 are still not elucidated compared to other pathogens of the order *Rickettsiales*. Indeed
485 *Rickettsia conorii* uses OmpA (Hillman et al., 2013) to adhere to the host cell whereas two
486 different receptors were described for *Anaplasma marginale* and *A. phagocytophilum*
487 mobilizing Msp1a and OmpA (de la Fuente et al., 2003), (Hebert et al., 2017), Asp14 and

488 OmpA (Kahlon et al., 2013), (Ojogun et al., 2012), respectively to attach cell membrane.
489 Adhesins and invasins were largely described in other bacteria as surface located structures
490 for specific interaction with host cell receptors (Niemann et al., 2004). *Yersinia* outer
491 membrane invasin interacts with ß1 integrin receptors, inducing several reactions including
492 actin rearrangements at the site of bacterial entry, promoting invasion. *Salmonella*
493 translocates several effectors into target cells, some of them allowing the initial uptake of
494 the bacterium, whereas *Listeria* uses InlA and InlB-dependent molecular pathways, (Pizarro-
495 Cerda and Cossart, 2006). Ligands often show elongated molecules containing domains
496 commonly found in eukaryotic proteins (Niemann et al., 2004).
497 We showed that rApe is O-glycosylated. Post-translational modifications are one of the most
498 important mechanisms for activating, changing, or suppressing protein functions, being
499 widely used by pathogens to interact with their hosts. *E. ruminantium* glycoproteomics
500 showed a high percentage of glycoproteins, many of them being O-glycosylated (Marcelino
501 et al., 2019). *E. ruminantium* “mucin”, which is also glycosylated, was presented as an
502 adhesin for tick cells, reinforcing a role of glycans in *Ehrlichia* adhesin molecules (de la
503 Fuente et al., 2004). The strength of ligand-receptor bacterial interactions is optimized
504 depending on their environment but weak enough to allow a bacterium to detach regularly
505 and migrate to other locations (Formosa-Dague et al., 2018). Glycan-glycan interactions in
506 bacterial-mammalian cells systems were characterized as low-affinity weak interactions
507 preceding high-affinity protein-glycan or protein-protein interactions but recent studies have
508 documented the importance of such interactions in bacterial adhesion (Formosa-Dague et
509 al., 2018). Indeed, we determined that the presence GAG on the surface of BAE plays a key
510 role in the attachment of *Ehrlichia* to bovine endothelial cells *in vitro*, reinforcing the
511 hypothesis that several receptors are probably required in *E. ruminantium* adhesion and
512 subsequent infection of host cells. Chondroitinase treatment significantly affected *Ehrlichia*
513 entry compared to the untreated condition. The enzymatic digestion of chondroitin and
514 dermatan from BAEC reduced the rate of infection of the BAEC, as *E. ruminantium* can no
515 longer adhere to the surface of the cells. Indeed, in other models like Chlamydia, GAGs
516 were shown to be used for initial attachment to host cells (Tiwari et al., 2012); Lyme disease
517 *Borreliae* requires glycosaminoglycan binding activity to colonize and disseminate to tissues
518 (Lin et al., 2017). Even though heparan sulfate appears to be the most important GAG
519 species involved in bacterial binding, both heparan sulfate and chondroitin sulfate were able
520 to influence the attachment of mucoid *P. aeruginosa, H. influenza* and *B. cepacia* in specific
521 ways that were dependent on the cell line involved (Martin et al., 2019). *Borrelia burgdorferi*

522 has multiple surface proteins with different binding specificities to GAGs depending on the
523 tissue affected (Leong et al., 1998). Different GAGs act as receptors for *B. burgdorferi*
524 depending on the host cells; both heparin sulfate and heparan sulfate are essential in
525 adherence to primary endothelium and adult kidney Vero cells, but only dermatan sulfate is
526 involved in attachment to human embryonic kidney cells (Garcia et al., 2016).
527 Although we did not establish the interaction of rApe adhesion with a cellular receptor, we
528 can still hypothesize that Ape actively triggers *Ehrlichia* internalization by the mean of a
529 ligand/receptor interaction. Kumar *et al*. already suggested the existence of additional
530 mammalian receptors for *Ehrlichia* infection (Mohan Kumar et al., 2013). The present study
531 identified the bacterial of a putative second *Ehrlichia* invasion-receptor pair and highlights
532 the importance of this molecular control of invasion for the *Anaplasmataceae* intracellular
533 bacteria. The probable existence of several ligand-receptor systems could indeed serve the
534 bacteria to infect a broader host range of animal reservoirs and vector ticks. Moreover, GAG
535 degradation following chondroitinase treatment severely impaired *Ehrlichia* infection. This
536 suggests that Ape could interact with a glycosylphosphatidylinositol (GPI)-anchored protein
537 as previously shown for PSGL-1 that is required for the binding and infection of human HL-
538 60 cells by *A. phagocytophylum* (Herron et al., 2000), This remains to be further studied as
539 well as its role in iron uptake of *Ehrlichia ruminantium* (Reneer et al., 2008).
540 In summary, with the identification of Ape (ERGA_CDS_01230), we found the first *Ehrlichia*
541 *ruminantium* protein that is involved in host cell invasion. Whether the *E. chaffeensis* EtpE
542 homolog (ERGA_CDS_08340) is functional in *E. ruminantium* remain to be explored, but
543 these outer-membrane proteins can now be considered as immune-dominant pathogen-
544 associated molecular patterns (Budachetri et al., 2020). Our next step is now to investigate
545 the use of rApe as a new vaccine candidate against Heartwater. In light of the lack of
546 prophylactic measures against *Ehrlichia* spp. and the rising appearance of antibiotic
547 resistances, deep understanding of invasion mechanisms is of prime importance and will
548 help to propose efficient alternative therapeutics blocking the early interaction between
549 these obligate intracellular bacteria and their host cells.
550

551 **Acknowledgements and funding information**

552 The authors acknowledge the financial support from Franco-Slovak bilateral project PHC
553 Stephanik 2014 n°31798XB and from European Union in the framework of the European
554 Regional Development Fund (ERDF), n° 2015-FED-186, MALIN project “Surveillance,
555 diagnosis, control and impact of infectious diseases of humans, animals and plants in

556 tropical islands”. We also gratefully acknowledge Géraldine Bossard and Valérie Rodrigues
557 for technical assistance in the development of ELISA assays.

558 # References

559 Allsopp, B.A. (2010). Natural history of Ehrlichia ruminantium. *Vet Parasitol* 167**,** 123-135.
560 Aquino, R.S., Lee, E.S., and Park, P.W. (2010). Diverse functions of glycosaminoglycans in infectious diseases. *Prog*
561 *Mol Biol Transl Sci* 93**,** 373-394.
562 Aquino, R.S., Teng, Y.H., and Park, P.W. (2018). Glycobiology of syndecan-1 in bacterial infections. *Biochem Soc Trans*.
563 Bartlett, A.H., and Park, P.W. (2010). Proteoglycans in host-pathogen interactions: molecular mechanisms and
564 therapeutic implications. *Expert Rev Mol Med* 12**,** e5.
565 Bioscience, J. (2011). LEXSinduce 3 Expression Kit for inducible expression of recombinant proteins in *Leishmania*
566 *tarentolae*. 28.
567 Brown, R.N., Romine, M.F., Schepmoes, A.A., Smith, R.D., and Lipton, M.S. (2010). Mapping the subcellular proteome
568 of Shewanella oneidensis MR-1 using sarkosyl-based fractionation and LC-MS/MS protein identification. *J*
569 *Proteome Res* 9**,** 4454-4463.
570 Budachetri, K., Teymournejad, O., Lin, M., Yan, Q., Mestres-Villanueva, M., Brock, G.N., and Rikihisa, Y. (2020). An
571 Entry-Triggering Protein of Ehrlichia Is a New Vaccine Candidate against Tick-Borne Human Monocytic
572 Ehrlichiosis. *mBio* 11.
573 Cangi, N., Gordon, J.L., Bournez, L., Pinarello, V., Aprelon, R., Huber, K., Lefrancois, T., Neves, L., Meyer, D.F., and
574 Vachiery, N. (2016). Recombination Is a Major Driving Force of Genetic Diversity in the Anaplasmataceae
575 Ehrlichia ruminantium. *Front Cell Infect Microbiol* 6**,** 111.
576 Cangi, N., Pinarello, V., Bournez, L., Lefrancois, T., Albina, E., Neves, L., and Vachiery, N. (2017). Efficient high-
577 throughput molecular method to detect *Ehrlichia ruminantium* in ticks. *Parasit Vectors* 10**,** 566.
578 Cheng, Z., Wang, X., and Rikihisa, Y. (2008). Regulation of type IV secretion apparatus genes during Ehrlichia
579 chaffeensis intracellular development by a previously unidentified protein. *J Bacteriol* 190**,** 2096-2105.
580 De La Fuente, J., Garcia-Garcia, J.C., Barbet, A.F., Blouin, E.F., and Kocan, K.M. (2004). Adhesion of outer membrane
581 proteins containing tandem repeats of *Anaplasma* and *Ehrlichia* species (Rickettsiales: *Anaplasmataceae*) to tick
582 cells. *Vet Microbiol* 98**,** 313-322.
583 De La Fuente, J., Garcia-Garcia, J.C., Blouin, E.F., and Kocan, K.M. (2003). Characterization of the functional domain
584 of major surface protein 1a involved in adhesion of the rickettsia *Anaplasma marginale* to host cells. *Vet*
585 *Microbiol* 91**,** 265-283.
586 Deem, S.L. (1998). A review of heartwater and the threat of introduction of Cowdria ruminantium and Amblyomma spp.
587 ticks to the American mainland. *J Zoo Wildl Med* 29**,** 109-113.
588 Delano, W.L. (2009). The PyMOL molecular graphics system.
589 .
590 Dumler, J.S., Barbet, A.F., Bekker, C.P., Dasch, G.A., Palmer, G.H., Ray, S.C., Rikihisa, Y., and Rurangirwa, F.R. (2001).
591 Reorganization of genera in the families *Rickettsiaceae* and *Anaplasmataceae* in the order Rickettsiales:
592 unification of some species of *Ehrlichia* with *Anaplasma*, *Cowdria* with *Ehrlichia* and *Ehrlichia* with
593 *Neorickettsia*, descriptions of six new species combinations and designation of Ehrlichia equi and 'HGE agent'
594 as subjective synonyms of *Ehrlichia phagocytophila*. *Int J Syst Evol Microbiol* 51**,** 2145-2165.
595 Formosa-Dague, C., Castelain, M., Martin-Yken, H., Dunker, K., Dague, E., and Sletmoen, M. (2018). The Role of
596 Glycans in Bacterial Adhesion to Mucosal Surfaces: How Can Single-Molecule Techniques Advance Our
597 Understanding? *Microorganisms* 6.
598 Frutos, R., Viari, A., Ferraz, C., Bensaid, A., Morgat, A., Boyer, F., Coissac, E., Vachiery, N., Demaille, J., and Martinez,
599 D. (2006). Comparative genomics of three strains of *Ehrlichia ruminantium*: a review. *Ann N Y Acad Sci* 1081**,**
600 417-433.
601 Frutos, R., Viari, A., Vachiery, N., Boyer, F., and Martinez, D. (2007). Ehrlichia ruminantium: genomic and evolutionary
602 features. *Trends Parasitol* 23**,** 414-419.
603 Gagoski, D., Mureev, S., Giles, N., Johnston, W., Dahmer-Heath, M., Skalamera, D., Gonda, T.J., and Alexandrov, K.
604 (2015). Gateway-compatible vectors for high-throughput protein expression in pro- and eukaryotic cell-free
605 systems. *J Biotechnol* 195**,** 1-7.
606 Garcia, B., Merayo-Lloves, J., Martin, C., Alcalde, I., Quiros, L.M., and Vazquez, F. (2016). Surface Proteoglycans as
607 Mediators in Bacterial Pathogens Infections. *Front Microbiol* 7**,** 220.
608 Green, R.S., Izac, J.R., Naimi, W.A., O'bier, N., Breitschwerdt, E.B., Marconi, R.T., and Carlyon, J.A. (2020). Ehrlichia
609 chaffeensis EplA Interaction With Host Cell Protein Disulfide Isomerase Promotes Infection. *Front Cell Infect*
610 *Microbiol* 10**,** 500.
611 Hebert, K.S., Seidman, D., Oki, A.T., Izac, J., Emani, S., Oliver, L.D., Jr., Miller, D.P., Tegels, B.K., Kannagi, R.,
612 Marconi, R.T., and Carlyon, J.A. (2017). Anaplasma marginale Outer Membrane Protein A Is an Adhesin That
613 Recognizes Sialylated and Fucosylated Glycans and Functionally Depends on an Essential Binding Domain.
614 *Infect Immun* 85.
615 Herron, M.J., Nelson, C.M., Larson, J., Snapp, K.R., Kansas, G.S., and Goodman, J.L. (2000). Intracellular parasitism by
616 the human granulocytic ehrlichiosis bacterium through the P-selectin ligand, PSGL-1. *Science* 288**,** 1653-1656.

Hillman, R.D., Baktash, Y.M., and Martinez, J.J. (2013). OmpA-mediated rickettsial adherence to and invasion of human endothelial cells is dependent upon interaction with alpha2beta1 integrin. *Cell Microbiol* 15**,** 727-741.

Jonquieres, R., Pizarro-Cerda, J., and Cossart, P. (2001). Synergy between the N- and C-terminal domains of InlB for efficient invasion of non-phagocytic cells by *Listeria monocytogenes*. *Mol Microbiol* 42**,** 955-965.

Kahlon, A., Ojogun, N., Ragland, S.A., Seidman, D., Troese, M.J., Ottens, A.K., Mastronunzio, J.E., Truchan, H.K., Walker, N.J., Borjesson, D.L., Fikrig, E., and Carlyon, J.A. (2013). *Anaplasma phagocytophilum* Asp14 is an invasin that interacts with mammalian host cells via its C terminus to facilitate infection. *Infect Immun* 81**,** 65-79.

Kobayashi, K., Kato, K., Sugi, T., Takemae, H., Pandey, K., Gong, H., Tohya, Y., and Akashi, H. (2010). *Plasmodium falciparum* BAEBL binds to heparan sulfate proteoglycans on the human erythrocyte surface. *J Biol Chem* 285**,** 1716-1725.

Leong, J.M., Robbins, D., Rosenfeld, L., Lahiri, B., and Parveen, N. (1998). Structural requirements for glycosaminoglycan recognition by the Lyme disease spirochete, Borrelia burgdorferi. *Infect Immun* 66**,** 6045-6048.

Lin, M., Liu, H., Xiong, Q., Niu, H., Cheng, Z., Yamamoto, A., and Rikihisa, Y. (2016). Ehrlichia secretes Etf-1 to induce autophagy and capture nutrients for its growth through RAB5 and class III phosphatidylinositol 3-kinase. *Autophagy* 12**,** 2145-2166.

Lin, Y.P., Li, L., Zhang, F., and Linhardt, R.J. (2017). *Borrelia burgdorferi* glycosaminoglycan-binding proteins: a potential target for new therapeutics against Lyme disease. *Microbiology* 163**,** 1759-1766.

Lundberg, M., Wikstrom, S., and Johansson, M. (2003). Cell surface adherence and endocytosis of protein transduction domains. *Mol Ther* 8**,** 143-150.

Marcelino, I., Colome-Calls, N., Holzmuller, P., Lisacek, F., Reynaud, Y., Canals, F., and Vachiery, N. (2019). Sweet and Sour Ehrlichia: Glycoproteomics and Phosphoproteomics Reveal New Players in Ehrlichia ruminantium Physiology and Pathogenesis. *Front Microbiol* 10**,** 450.

Marcelino, I., Verissimo, C., Sousa, M.F., Carrondo, M.J., and Alves, P.M. (2005). Characterization of *Ehrlichia ruminantium* replication and release kinetics in endothelial cell cultures. *Vet Microbiol* 110**,** 87-96.

Martin, C., Lozano-Iturbe, V., Giron, R.M., Vazquez-Espinosa, E., Rodriguez, D., Merayo-Lloves, J., Vazquez, F., Quiros, L.M., and Garcia, B. (2019). Glycosaminoglycans are differentially involved in bacterial binding to healthy and cystic fibrosis lung cells. *J Cyst Fibros* 18**,** e19-e25.

Martinez, D., Coisne, S., Sheikboudou, C., and Jongejan, F. (1993). Detection of antibodies to Cowdria ruminantium in the serum of domestic ruminants by indirect ELISA. *Rev Elev Med Vet Pays Trop* 46**,** 115-120.

Martinez, E., Cantet, F., Fava, L., Norville, I., and Bonazzi, M. (2014). Identification of OmpA, a *Coxiella burnetii* protein involved in host cell invasion, by multi-phenotypic high-content screening. *PLoS Pathog* 10**,** e1004013.

Martinez, J.J., Seveau, S., Veiga, E., Matsuyama, S., and Cossart, P. (2005). Ku70, a component of DNA-dependent protein kinase, is a mammalian receptor for Rickettsia conorii. *Cell* 123**,** 1013-1023.

Miller, E.M., and Nickoloff, J.A. (1995). *Escherichia coli* electrotransformation. *Methods Mol Biol* 47**,** 105-113.

Mohan Kumar, D., Yamaguchi, M., Miura, K., Lin, M., Los, M., Coy, J.F., and Rikihisa, Y. (2013). *Ehrlichia chaffeensis* uses its surface protein EtpE to bind GPI-anchored protein DNase X and trigger entry into mammalian cells. *PLoS Pathog* 9**,** e1003666.

Moumene, A., Gonzalez-Rizzo, S., Lefrancois, T., Vachiery, N., and Meyer, D.F. (2017). Iron Starvation Conditions Upregulate *Ehrlichia ruminantium* Type IV Secretion System, tr1 Transcription Factor and map1 Genes Family through the Master Regulatory Protein ErxR. *Front Cell Infect Microbiol* 7**,** 535.

Moumene, A., Marcelino, I., Ventosa, M., Gros, O., Lefrancois, T., Vachiery, N., Meyer, D.F., and Coelho, A.V. (2015). Proteomic profiling of the outer membrane fraction of the obligate intracellular bacterial pathogen *Ehrlichia ruminantium*. *PLoS One* 10**,** e0116758.

Moumene, A., and Meyer, D.F. (2015). *Ehrlichia*'s molecular tricks to manipulate their host cells. *Microbes Infect*.

Niemann, H.H., Schubert, W.D., and Heinz, D.W. (2004). Adhesins and invasins of pathogenic bacteria: a structural view. *Microbes Infect* 6**,** 101-112.

Noroy, C., Lefrancois, T., and Meyer, D.F. (2019). Searching algorithm for Type IV effector proteins (S4TE) 2.0: Improved tools for Type IV effector prediction, analysis and comparison in proteobacteria. *PLoS Comput Biol* 15**,** e1006847.

Ojogun, N., Kahlon, A., Ragland, S.A., Troese, M.J., Mastronunzio, J.E., Walker, N.J., Viebrock, L., Thomas, R.J., Borjesson, D.L., Fikrig, E., and Carlyon, J.A. (2012). *Anaplasma phagocytophilum* outer membrane protein A interacts with sialylated glycoproteins to promote infection of mammalian host cells. *Infect Immun* 80**,** 3748-3760.

Perez, J.M., Martinez, D., Sheikboudou, C., Jongejan, F., and Bensaid, A. (1998). Characterization of variable immunodominant antigens of *Cowdria ruminantium* by ELISA and immunoblots. *Parasite Immunol* 20**,** 613-622.

Pizarro-Cerda, J., and Cossart, P. (2006). Bacterial adhesion and entry into host cells. *Cell* 124**,** 715-727.

Pruneau, L., Emboule, L., Gely, P., Marcelino, I., Mari, B., Pinarello, V., Sheikboudou, C., Martinez, D., Daigle, F.,

677 Lefrancois, T., Meyer, D.F., and Vachiery, N. (2012). Global gene expression profiling of *Ehrlichia ruminantium*
678 at different stages of development. *FEMS Immunol Med Microbiol* 64**,** 66-73.
679 Rajas, O., Quiros, L.M., Ortega, M., Vazquez-Espinosa, E., Merayo-Lloves, J., Vazquez, F., and Garcia, B. (2017).
680 Glycosaminoglycans are involved in bacterial adherence to lung cells. *BMC Infect Dis* 17**,** 319.
681 Reneer, D.V., Troese, M.J., Huang, B., Kearns, S.A., and Carlyon, J.A. (2008). Anaplasma phagocytophilum PSGL-1-
682 independent infection does not require Syk and leads to less efficient AnkA delivery. *Cell Microbiol* 10**,** 1827-
683 1838.
684 Rikihisa, Y. (2017). Role and Function of the Type IV Secretion System in Anaplasma and Ehrlichia Species. *Curr Top*
685 *Microbiol Immunol* 413**,** 297-321.
686 Sava, I.G., Zhang, F., Toma, I., Theilacker, C., Li, B., Baumert, T.F., Holst, O., Linhardt, R.J., and Huebner, J. (2009).
687 Novel interactions of glycosaminoglycans and bacterial glycolipids mediate binding of enterococci to human
688 cells. *J Biol Chem* 284**,** 18194-18201.
689 Teymournejad, O., Lin, M., and Rikihisa, Y. (2017). Ehrlichia chaffeensis and Its Invasin EtpE Block Reactive Oxygen
690 Species Generation by Macrophages in a DNase X-Dependent Manner. *mBio* 8.
691 Tiwari, V., Maus, E., Sigar, I.M., Ramsey, K.H., and Shukla, D. (2012). Role of heparan sulfate in sexually transmitted
692 infections. *Glycobiology* 22**,** 1402-1412.
693 Truttmann, M.C., Rhomberg, T.A., and Dehio, C. (2011). Combined action of the type IV secretion effector proteins
694 BepC and BepF promotes invasome formation of Bartonella henselae on endothelial and epithelial cells. *Cell*
695 *Microbiol* 13**,** 284-299.
696 Waterhouse, A., Bertoni, M., Bienert, S., Studer, G., Tauriello, G., Gumienny, R., Heer, F.T., De Beer, T.a.P., Rempfer,
697 C., Bordoli, L., Lepore, R., and Schwede, T. (2018). SWISS-MODEL: homology modelling of protein structures
698 and complexes. *Nucleic Acids Res* 46**,** W296-W303.
699 Xiaogen Zhou, W.Z., Yang Li, Robin Pearce, Chengxin Zhang, Eric W. Bell, Guijun Zhang, and Yang Zhang (2022). I-
700 TASSER-MTD: A deep-learning based platform for multi-domain protein structure and function prediction.
701 *Nature Protocols, in press*.
702 Yan, Q., Lin, M., Huang, W., Teymournejad, O., Johnson, J.M., Hays, F.A., Liang, Z., Li, G., and Rikihisa, Y. (2018).
703 Ehrlichia type IV secretion system effector Etf-2 binds to active RAB5 and delays endosome maturation. *Proc*
704 *Natl Acad Sci U S A* 115**,** E8977-E8986.
705 Yang, J., and Zhang, Y. (2015). I-TASSER server: new development for protein structure and function predictions.
706 *Nucleic Acids Res* 43**,** W174-181.
707 Yu, C.S., Chen, Y.C., Lu, C.H., and Hwang, J.K. (2006). Prediction of protein subcellular localization. *Proteins* 64**,** 643-
708 651.
709

710 ## Figure captions

711 **Figure 1. Temporal expression of the (ERGA_CDS_01230) *ape* gene in *E. ruminantium***
712 **determined by qRTPCR.**

713 (A) *E. ruminantium* sigmoïdal growth curve was determined by qPCR targeting *pCS20*
714 region and represented as relative bacterial number along the cycle of development
715 (B) Transcript levels were determined from 24, 48, 72 and 120 hpi by qRTPCR targeting
716 ERGA_CDS_01230 gene. Levels were normalized by the quantity of bacteria measured by
717 qPCR Sol1 and the ratio was compared to 96 hpi, allowing fold-change (FC) determination,
718 expressed as log 2. Values at each time point are the means +/- standard deviations for 2
719 biological replicates. Gp38 is for *E. ruminantium* Gardel strain, passage #38 (virulent strain).
720

721 **Figure 2. Structural characterization of Ape protein.**

722 (A-H) I-TASSER-MTD derived 3D-prediction of the ERGA_CDS_01230 gene product (Ape
723 protein in green) interacting with oxo-iron molecule (red). Front (A-B), back (C-D) and side
724 (E-F) views of Ape showing a succession of α-helixes (turquoise) linked by loops (pink)
725 distributed around β-sheets (purple), organized as a three-dimensional “c-clamp” structure.
726 The enlarged panels (G-H) of the binding site allow the visualization of the residues involved
727 in polar (yellow) and non-polar (light blue) interactions. The oxo-iron molecule (CIN1)
728 constituted by 3 atoms of iron (orange) and 12 atoms of oxygen (red) interacts with Ape
729 protein (green) via polar interaction (hydrogen bond with T99 in yellow) and non-polar
730 interactions (hydrophobic interactions in light blue involving L120 and Q122) bonds.
731 (I) Reliability score prediction by CELLO 2.5 software of the subcellular localization of the
732 native *E. ruminantium* Ape protein. Ape presents a typical subcellular localization of an
733 active transporter, with a dominant cytoplasmic localization and is also present at the outer
734 membrane.
735

736 **Figure 3. rApe is an O-glycosylated recombinant protein.**

737 Composite picture of a Western blot detecting O-glycosylation of recombinant Ape protein
738 (lane 2). Recombinant proteins were separated by SDS-PAGE, then transferred to PVDF
739 and incubated with anti-O-GlcNAc antibody. The Western blot was probed with anti-mouse
740 IgM-HRP antibody and revealed by TMB substrate. Lane 1: negative control : BSA; lane 2:
741 rApe. Numbers and black arrowheads indicate molecular masses in kilodaltons (kDa). The
742 recognized rApe is significantly larger (66 kDa) than the one predicted by the amino acid
743 sequences encoded by ERGA_CDS_01230 gene (41 kDa).

744

745 **Figure 4**. **Chondroitinase impairs BAEC infection by *E. ruminantium*.** Using 0.4 and
746 0.9U/mL chondroitinase resulted in a halving of the number of bacteria compared to the
747 untreated condition. Bacterial quantification was performed at lysis stage by qPCR sol1 after
748 chondroitinase treatment at three different concentration. Fold-change (FC) was obtained
749 by calculating the bacterial amount differential for each condition compared to the condition
750 without treatment and represented as $2^{-\Delta\Delta Ct}$.

751

752 **Figure 5. rApe attaches to the host cells.**
753 Different concentrations of rApe tagged with GFP were incubated with BAEC. Adherence of
754 GFP-rApe to prefixed BAEC was evaluated by flow cytometry and showed a dose-effect
755 relationship up to 36 µg of rApe. Fluorescent-labelled cells quantified by flow cytometry are
756 represented in % for each concentration point. Auto-fluorescence was evaluated with cells
757 without recombinant protein.

758

759 **Figure 6. rApe interacts with cell lysate and membrane fractions.**
760 Composite picture of a Far-Western blot detecting Ape protein. Lysate and cell fractions
761 were separated by SDS-PAGE, transferred to PVDF and incubated either with rApe (left
762 panel) or PBS as a negative control (right panel). The Western blot was probed with rabbit
763 anti-GFP-HRP antibody, and revealed by peroxide substrate mixed with chromogen DAB.
764 1: protein ladder, 2 and 5: cell lysate, 3: cytoskeleton fraction, 4 and 6: membrane and
765 organelles fraction.

766

767 **Figure 7. rApe is sufficient for adhesion of latex beads to bovine endothelial cells.**
768 Representative images of BAEC incubated 30 minutes with fluorescent latex beads
769 (1.82×10^8) coated with rApe and processed for scanning electron microscopy.
770 (A) Endothelial cells did not retain non-adsorbed beads (0.1µm diameter) on their cell
771 surface. (B) On the opposite, the whole surface of the same type of cells are covered with
772 adherent beads (0.5µm diameter) absorbed with rApe. (C) Enlarged view of adherent beads.
773 Such beads present two kinds of localizations. Some of them are already internalized (black
774 arrow heads) while others are still located outside the cell remaining in contact with the
775 cytoplasmic membrane (white arrow heads). Scale bars are indicated.

776

777 **Figure 8. Ape induces an antibody response in sera of vaccinated goats.**

778 The antibody response to Ape during vaccination kinetic was tested by ELISA. Sera of
779 vaccinated goats were incubated in wells coated with rApe, followed by incubation with anti-
780 goat antibody coupled to HRP. Antibody response was detected by ELISA titers (optical
781 density at 450 nm). Shown are representative results from five vaccinated goats. #614: goat
782 vaccinated with an attenuated vaccine. #915: goat vaccinated with an inactivated vaccine.
783 The time (in weeks) post-vaccination is indicated. Goats vaccinated with inactivated vaccine
784 were also challenged for resistance to *E. ruminantium* Gardel strain seven weeks post
785 vaccination.
786
787 **Figure 9. Schematic representation of *Ehrlichia ruminantium* binding to mammalian**
788 **cells and rApe interaction with the host cell surface**.
789 Ape is located at *E. ruminantium* outer membrane and is recognized by antibody from sera
790 of vaccinated animals. *E. ruminantium* can adhere and enter into BAEC but infection is
791 reduced when GAG like chondroitin and dermatan sulfate are degraded. The recombinant
792 version of *E. ruminantium*, rApe, is glycosylated and latex beads coated with rApe bind to
793 BAE cell surface and start to enter in BAEC, in a similar manner that of *E. ruminantium.*
794 Whether Ape binds to a cellular receptor and the following triggered signaling cascade
795 remain to be determined.

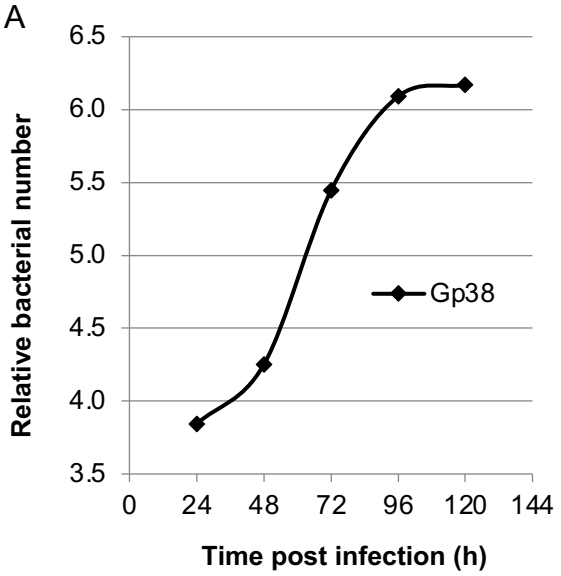
A
6.5
6.0
5.5
5.0
4.5
4.0
3.5
Relative bacterial number
Gp38
0
24
48
72
96
120
144
Time post infection (h)

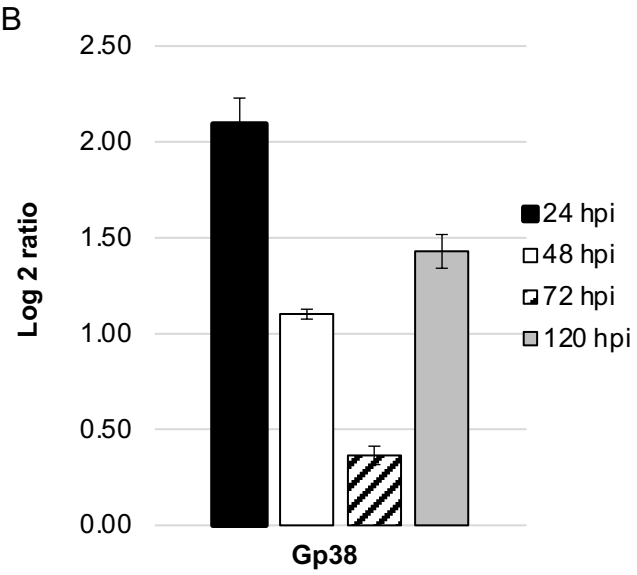
B
2.50
2.00
1.50
1.00
0.50
0.00
Log 2 ratio
24 hpi
48 hpi
72 hpi
120 hpi
Gp38

Figure 1

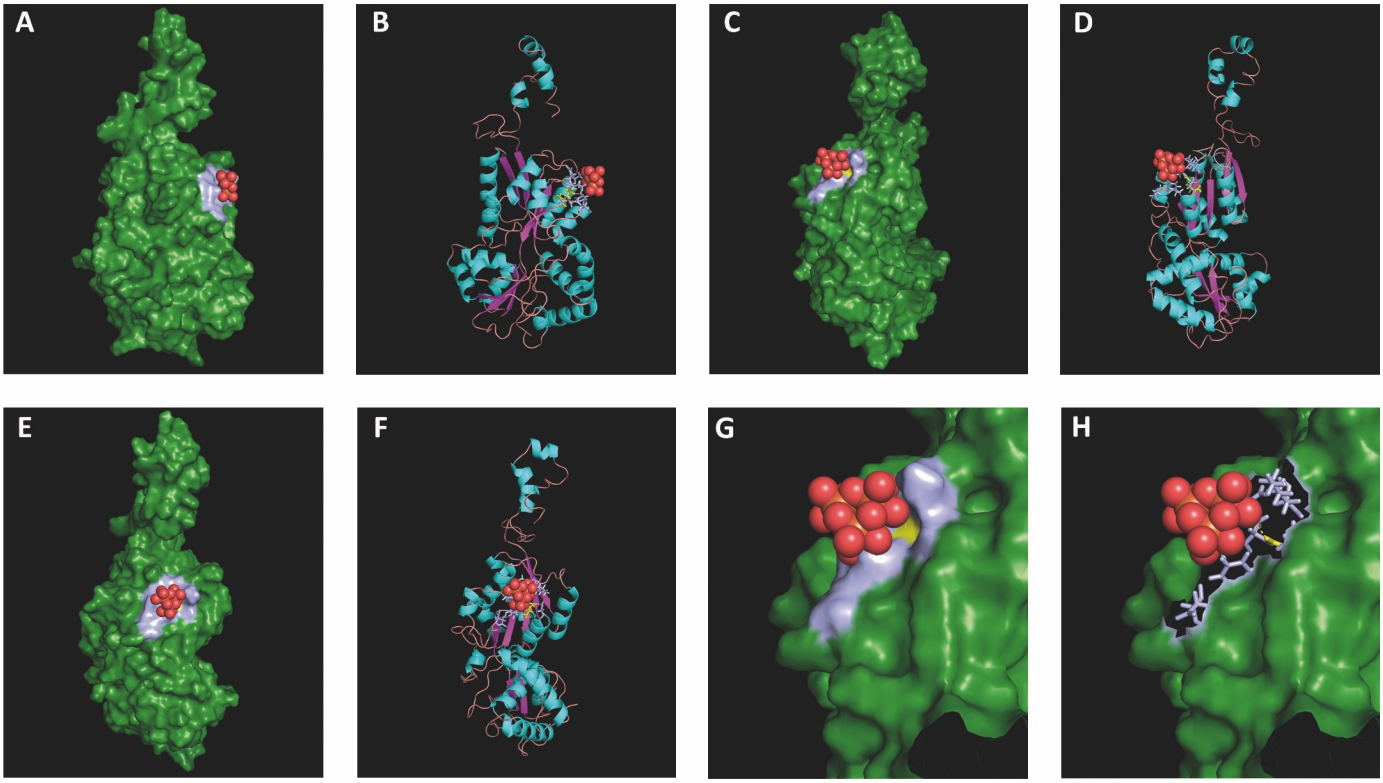

I

BACTERIAL LOCALIZATION	ERGA_CDS_01230
Cytoplasmic	**2,418**
Outer membrane	**1,652**
Periplasmic	0,424
Inner membrane	0,404
Extracellular	0,102

Figure 2

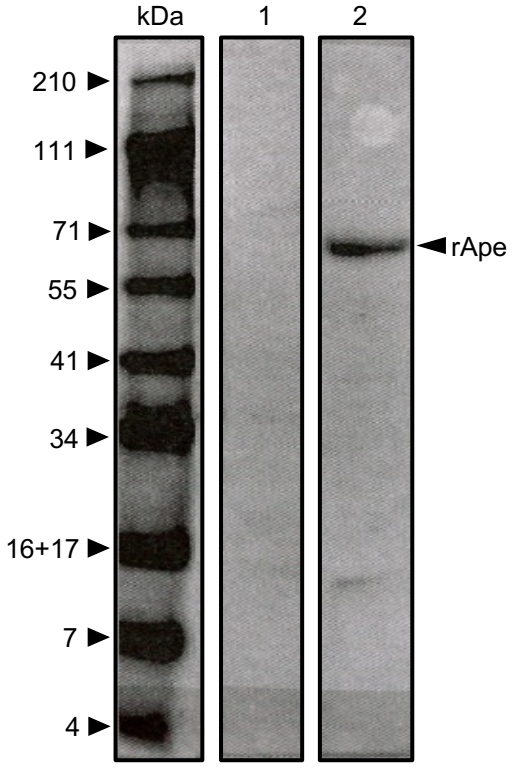

Figure 3

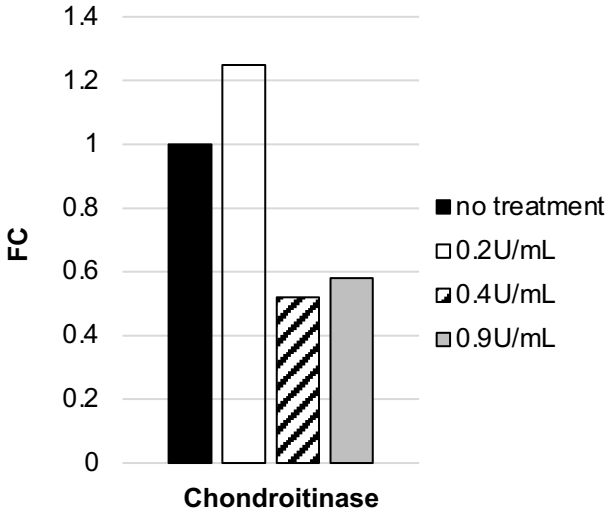
1.4
1.2
1
0.8
0.6
0.4
0.2
0
FC
Chondroitinase
no treatment
0.2U/mL
0.4U/mL
0.9U/mL

Figure 4

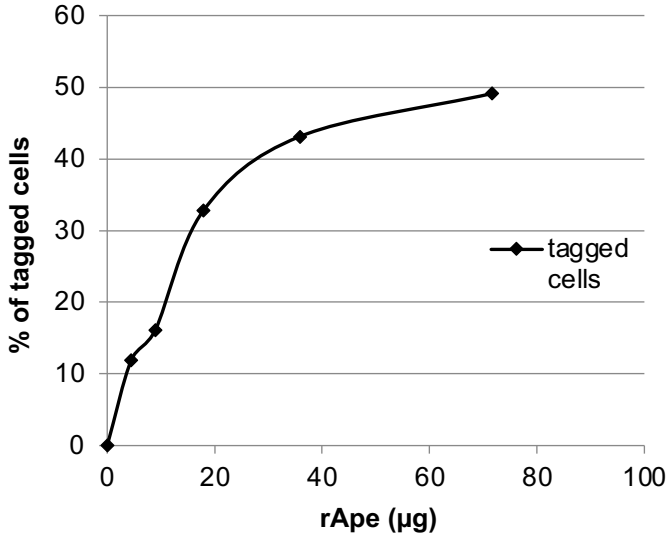
60
50
40
30
20
10
0
% of tagged cells
0
20
40
60
80
100
rApe (µg)
tagged cells

Figure 5

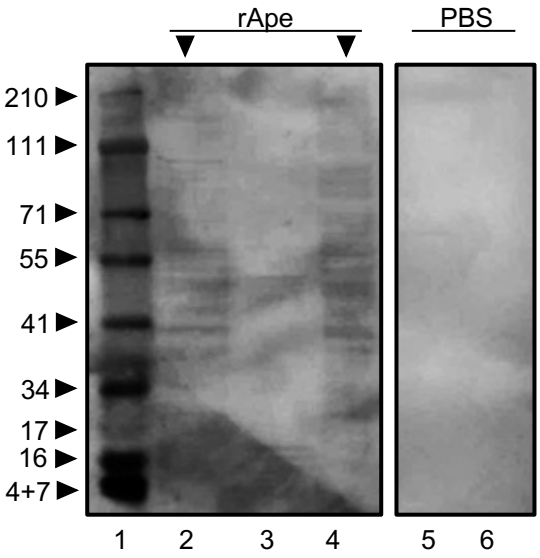

Figure 6

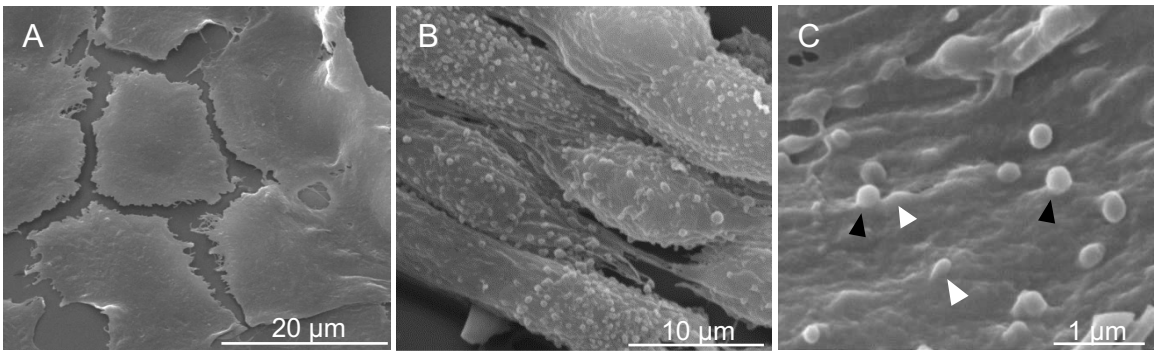

Figure 7

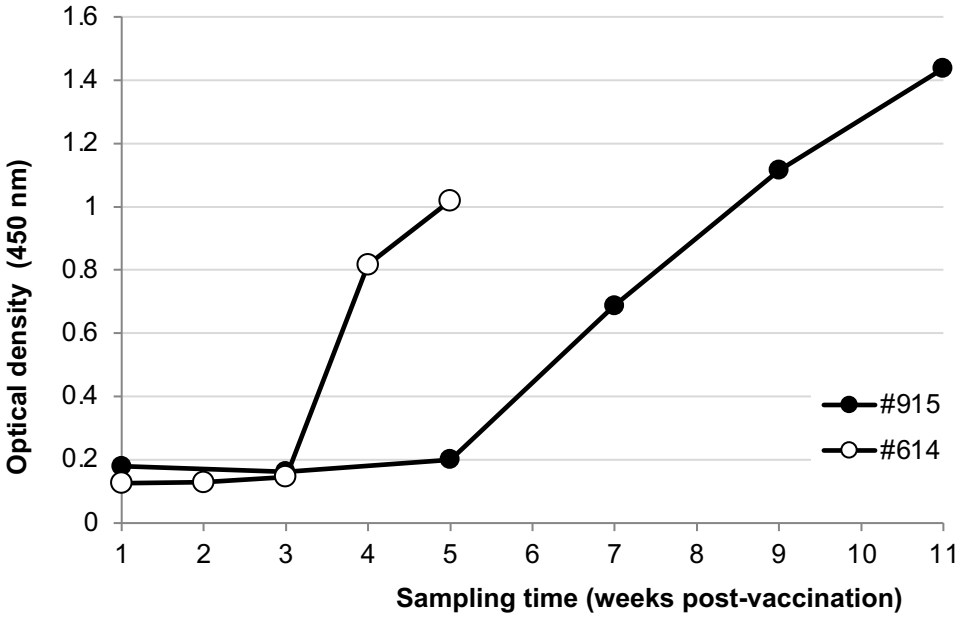
1.6
1.4
1.2
1
0.8
0.6
0.4
0.2
0
Optical density (450 nm)
1
2
3
4
5
6
7
8
9
10
11
Sampling time (weeks post-vaccination)
#915
#614

Figure 8

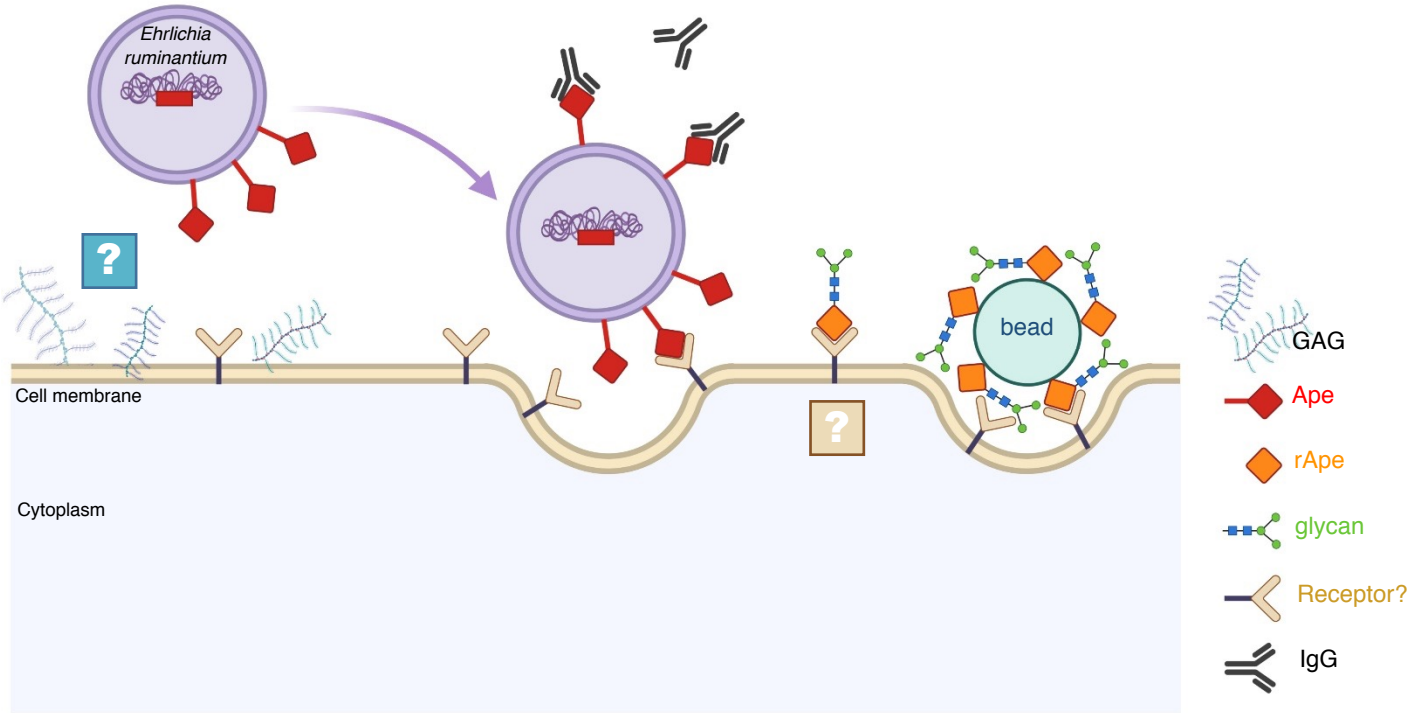
Ehrlichia ruminantium
?
Cell membrane
Cytoplasm
?
bead
GAG
Ape
rApe
glycan
Receptor?
IgG